Extended Stoner factor calculations for the half-metallic ferromagnets NiMnSb and CrO_2

1990 J. Phys.: Condens. Matter 2 343

(http://iopscience.iop.org/0953-8984/2/2/010)

J. Phys.: Condens. Matter 2 (1990) 343–350. Printed in the UK

Extended Stoner factor calculations for the half-metallic ferromagnets NiMnSb and CrO_2

E Kulatov† and I I Mazin‡§

† Institute of General Physics, Moscow 117924, GSP-1, USSR

‡ Max-Planck-Institut für Festkörperforschung, Heisenbergstrasse 1, D7000 Stuttgart-80, Federal Republic of Germany

Received 30 May 1989

Abstract. The electronic structures of NiMnSb and CrO_2 were calculated using a spin-polarised scalar relativistic linear muffin-tin orbital (LMTO) method. The self-consistent calculations were performed for the observed experimental lattice constants. Cubic NiMnSb (MgAgAs-type structure) and rutile-structure CrO_2 are found to be 'half-metallic ferromagnets', i.e. they have a semiconducting gap in the minority-spin bands but metallic majority-spin bands. The calculated magnetic moments in both compounds were found to be in good agreement with the experimental values. The possibility of metastable magnetic states is investigated via extended Stoner factor calculations. It is shown that the position of the Fermi level with respect to the band gap is extremely sensitive to the exchange–correlation potential approximation.

1. Introduction

A few years ago de Groot *et al* (1983) drew attention to Mn-based Heusler alloys which had been shown to have a peculiar band structure—that is, they were found to have a gap in the minority-spin sub-bands and to show normal metallic behaviour as regards the majority-spin bands. This means, in particular, that electrons at the Fermi level are 100% spin-polarised. Such materials were called, in that paper, 'half-metallic ferromagnets' (HMF). Later other materials of this kind were found, for instance CrO_2 (Schwarz 1986). These HMF are also interesting because of a large magneto-optical Kerr effect, which is characteristic of these compounds. It is very probable that magneto-optical properties of HMF are closely related to the presence of the gap in one of the spin sub-bands (de Groot *et al* 1984).

In connection with this, some interesting questions arise, which we try to answer in the following paper. First, is it possible to find out from a *non-magnetic* calculation whether a particular material is a HMF, as one can find a ferromagnetic instability in non-magnetic Stoner factor calculations? Second, how accurate are state-of-the-art *spin-polarised* band structure calculations in determining the relative position of the Fermi level inside the spin-down band gap? The last question is especially important from the magneto-optical point of view. In the following we shall discuss two materials: NiMnSb and CrO_2.

2. Crystal structures

The intermetallic compound NiMnSb crystallises in a cubic structure of MgAgAs type with the FCC Bravais lattice (space group: $F\bar{4}3m = T_d^2$). This structure can be described

§ Permanent address: P N Lebedev Physical Institute, Moscow 11794, GSP-1, USSR.

0953-8984/90/020343 + 08 $03.50

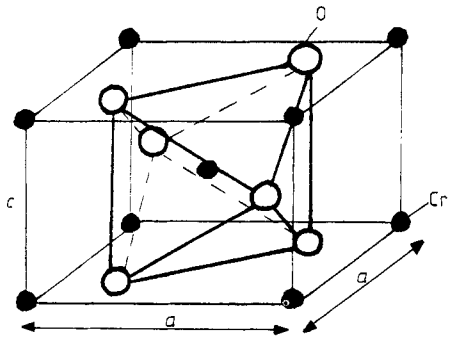

Figure 1. Crystal structure of CrO_2.

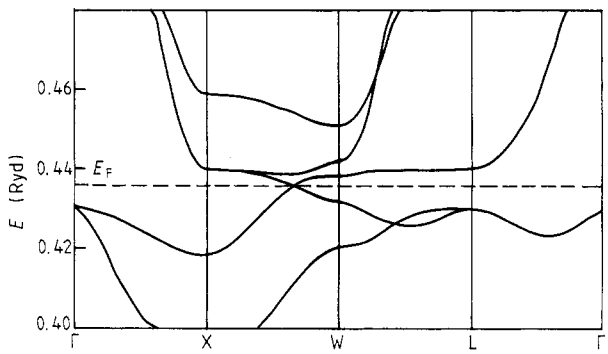

Figure 2. Non-magnetic band structure of NiMnSb.

as three interpenetrating FCC lattices of Ni, Mn and Sb. The Mn and Sb sublattices are shifted relative to the Ni sublattice by a quarter of the (111) diagonal in opposite directions.

Chromium dioxide, CrO_2, has the rutile-type (tetragonal) crystal structure with a = 4.421 Å and c/a = 0.659 58. The Cr atoms form a body-centred tetragonal lattice and are surrounded by a slightly distorted octahedron of oxygen atoms (figure 1). The space group of this compound is non-symmorphic ($P4_2/mnm = D_{4h}^{14}$)

3. Calculational method

We have performed self-consistent scalar relativistic spin-polarised (as well as non-magnetic) calculations of the band structures of NiMnSb and CrO_2. The present calculations were carried out using the LMTO method (Andersen 1975). The Janak–Moruzzi–Williams (1975) exchange–correlation potential was used. To achieve self-consistency, 88 (75) k-points in the irreducible wedge of the MgAgAs (rutile) Brillouin zone were used. Because of the openness of the crystal structures the combined correction terms and additional empty sphere (in the case of NiMnSb) are necessary. Empty spheres in between Mn and Sb were used for NiMnSb. The density-of-states (DOS) functions were obtained using the tetrahedron method. The core states were frozen during the self-consistent iterations for the valence states. The experimental lattice constants (Watanabe 1976, Kamper *et al* 1987) were used in both cases. For CrO_2 we

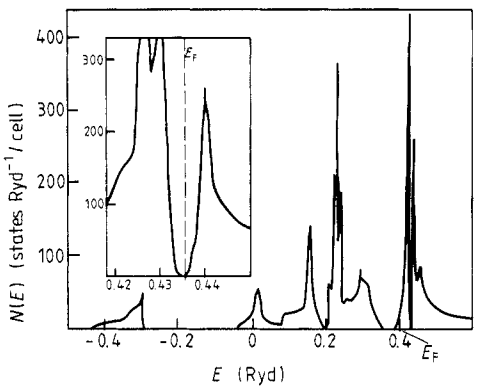

Figure 3. Density of states corresponding to the band structure shown in figure 2.

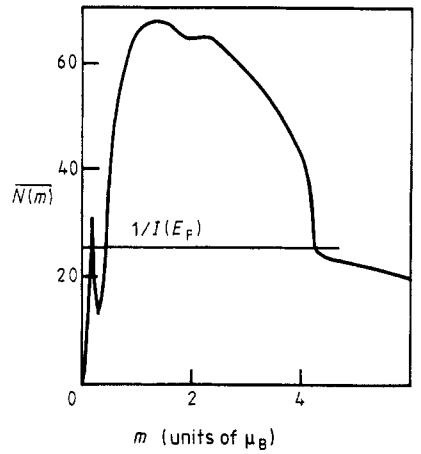

Figure 4. Extended Stoner factor calculations for NiMnSb.

have used equal atomic spheres for Cr and O with the radii 2.483 au. For NiMn(empty)Sb the sphere radii were chosen as 2.892, 2.892, 1.446 and 3.181 au, so the radii ratios are 1:1:0.5:1.1.

4. Results and discussion

4.1. NiMnSb

In figures 2 and 3 we show the band structure and corresponding DOS functions of non-magnetic NiMnSb. The lower valence bands in figure 3 have been omitted to show the region around the Fermi level (E_F) in greater detail. The striking feature seen in the non-magnetic NiMnSb band structure is the negligibly small DOS at E_F (see also figure 3 and table 1). In all high-symmetry directions the Fermi level falls within the narrow gap except for in the X–W direction where there is an accidental crossing of two bands. The self-consistent position of E_F necessarily coincides with this point because exactly 11 bands are to be filled to attain 22 electrons per unit cell. Hence, paramagnetic NiMnSb would be a zero-gap semiconductor with zero DOS at the Fermi level. However, away from the Fermi level the DOS is rapidly increasing.

The valence states separate into four regions each of which is of one predominant orbital character, and thus we may refer to them as Sb 5s, Sb 5p, Ni 3d and Mn 3d bands. Naturally, as a consequence of the hybridisation effects, some contributions from alien electron states are present in each region. The Fermi level cuts the Mn 3d bands, the Mn e_g states being located below E_F and the Mn t_{2g} states above E_F.

Because of the vanishing DOS at E_F, the simple Stoner theory evidently fails for NiMnSb, as the Stoner factor $N(E_F)^*I$ also vanishes. This is not so, however, for the extended Stoner factor calculations (ESFC) (Andersen *et al* 1977, Krasko 1987). The idea of ESFC is to calculate the average DOS as a function of magnetic moment m in the rigid-band approximation $\overline{N(m)} = m/\Delta E$, where ΔE is the spin splitting of the bands at the Fermi level. The results of our ESFC are shown in figure 4. The Stoner integral I was calculated after Gunnarsson (1976). It may be shown (Andersen *et al* 1977, Krasko 1987) that (meta)stable states correspond to $\overline{N(m)} = 1/I$. In the case of NiMnSb, we have one

Table 1. Band structure parameters for NiMnSb.

	Ferromagnetic phase					Non-magnetic phase			
	n_s	n_p	n_d	M	q	n_s	n_p	n_d	q
↑	0.383	0.542	4.678						
Ni				0.181	+1.025	0.782	1.104	9.178	+1.067
↓	0.394	0.592	4.436						
↑	0.298	0.335	4.647						
Mn				3.926	−0.367	0.481	0.558	5.625	−0.337
down	0.231	0.284	0.838						
↑	0.023	0.010	—						
Empty				0.002	+0.063	0.056	0.022	—	+0.077
↓	0.021	0.009	—						
↑	0.772	1.316	—						
Sb				−0.106	−0.719	1.514	2.679	—	−0.808
↓	0.759	1.434	—						

$m_{theor} = 4.004\mu_B$, $m_{exp} = 3.850\mu_B$
$N(E_F) = 10.723$ states Ryd^{-1}/cell

$I(E_F) = 0.045$ Ryd for Mn 3d
$N(E_F) = 0.0$ states Ryd^{-1}/cell

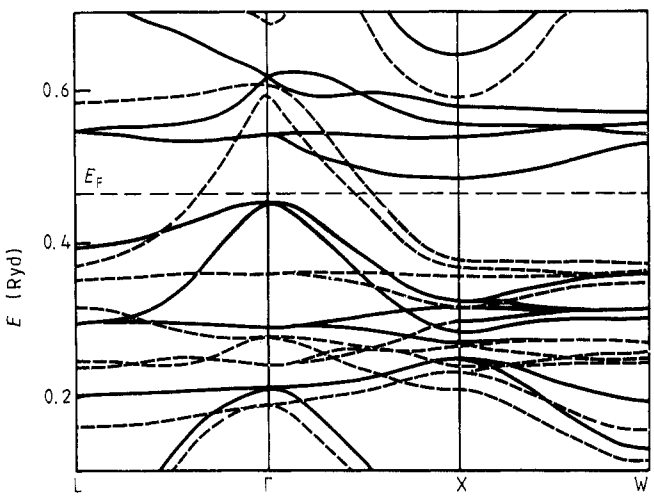

Figure 5. Spin-polarised band structure of NiMnSb. Exchange–correlation potential after von Barth and Hedin (1972). Broken curves show spin-up bands.

metastable low-spin solution ($m = 0.14\mu_B$) and one stable high-spin solution. An interesting feature is a step-like singularity in the $\overline{N(m)}$ dependence at $m = 4\mu_B$. This is due to the fact that at $m = 4\mu_B$ a gap opens in the minority-spin band because the e_g minority band is now empty, and the further increase in splitting does not change the magnetic moment while $\overline{N(m)}$ is decreasing. After some critical value, a further increase in splitting must cause an increase in magnetic moment. It is not surprising that the intersection of the curve $\overline{N(m)}$ with the line $1/I$ is exactly at $m = 4\mu_B$, because this value of m corresponds to the entire region of $1/I$ from $\simeq 22$ to $\simeq 38$ Ryd^{-1}. However, the position of the Fermi level inside the gap is difficult to determine accurately in the

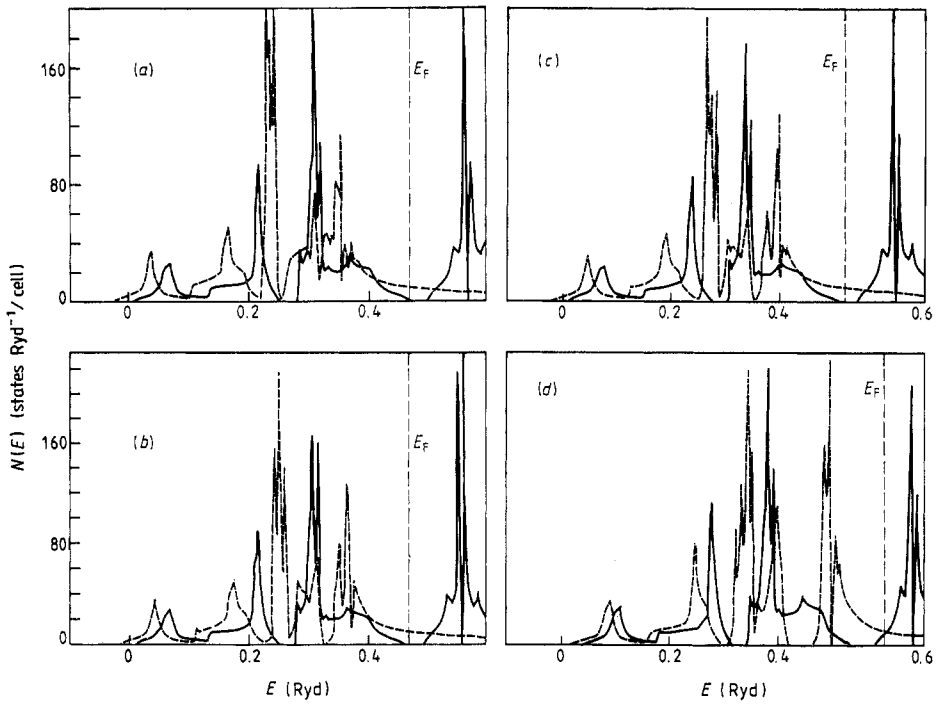

Figure 6. Density of states of ferromagnetic NiMnSb. Broken traces show spin-up DOS. Exchange–correlation potential after (*a*) Janak *et al* (1975), (*b*) von Barth and Hedin (1972), (c) Gunnarsson and Lundqvist (1976), (*d*) Vosko *et al* (1980). In all cases the corresponding exchange–correlation potential was used throughout the whole self-consistency procedure.

framework of the rigid-band approximation. In figure 4 the intersection at $m = 4\mu_B$ occurs somewhere between the largest and the smallest values of $\overline{N(m)}$, but nearer to the smallest; this means that the Fermi level should fall somewhere inside the gap, near the bottom. Indeed, our self-consistent spin-polarised band structure calculations for NiMnSb (figures 5, 6) show that in fact E_F is situated near the bottom of the gap, when we use the Janak–Moruzzi–Williams (1975) approximation for the exchange–correlation potential. However, the self-consistent position of E_F inside the gap is extremely sensitive to the exchange–correlation approximation used (cf figure 6). When we used the von Barth–Hedin (1972) approximation, E_F turned out to be in the middle of the gap; using the Gunnarsson–Lundqvist (1976) approximation moved E_F further to the bottom of the gap. In the Vosko–Wilk–Nussair (1980) approximation E_F is situated exactly at the top (see figure 6).

Such sensitivity seems at first sight very unusual, as normally only small details of the band structure are affected by changing the exchange–correlation approximation. It should be noted, however, that the difference in the exchange splitting in different approximations is not too large here. However, while the gap itself is small in comparison with the exchange splitting, the relative position of E_F inside the gap is much affected by the choice of exchange–correlation approximation. To move E_F away from the gap is, however, more difficult, since this would be accompanied by a change in the magnetic moment. This can also be explained on the basis of the fact that in the rigid-band approximation, i.e. in ESFC, the total energy does not depend at all on the position of the Fermi level as long as it lies anywhere inside the gap, but the value of the magnetic

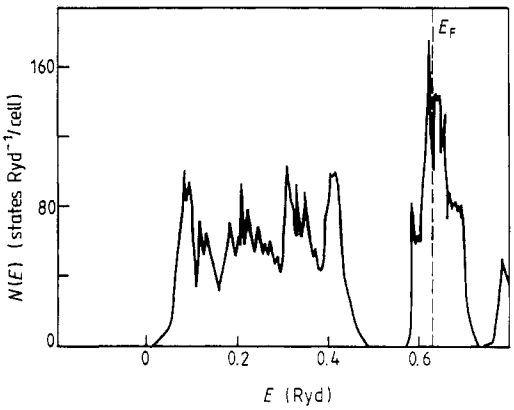

Figure 7. Non-magnetic density of states of CrO_2.

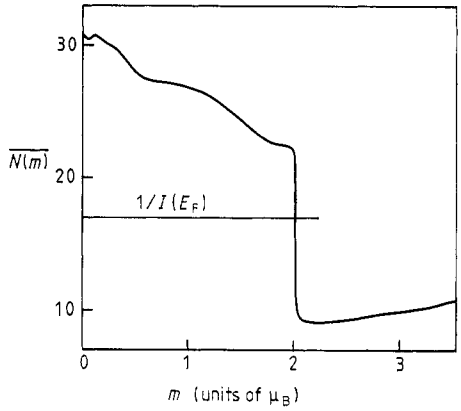

Figure 8. Extended Stoner factor calculations for CrO_2.

Table 2. Band structure parameters for CrO_2 calculated using the Janak–Moruzzi–Williams exchange–correlation potential.

	Ferromagnetic phase					Non-magnetic phase			
	n_s	n_p	n_d	M	q	n_s	n_p	n_d	q
↑	0.212	0.366	2.786						
Cr				1.945	−1.099	0.375	0.622	3.947	−1.062
↓	0.199	0.352	0.867						
↑	0.909	2.409	—						
O				0.028	+0.550	1.831	4.697	—	+0.531
↓	0.907	2.383	—						
$m_{theor} = 1.972\mu_B$, $m_{exp} = 2.01\mu_B$						$I(E_F) = 0.058$ Ryd for Cr 3d			
$N(E_F) = 63.71$ states Ryd^{-1}/cell						$N(E_F) = 149.62$ states Ryd^{-1}/cell			

moment is strictly fixed. De Groot *et al* (1983, 1984) have found E_F well inside the gap for NiMnSb and near the bottom of the gap for PtMnSb. They believe that it is this difference that causes the magneto-optical Kerr effect to be much higher in PtMnSb. We believe, however, that the position of the Fermi level with respect to the gap cannot be reliably determined from the LDA calculations with the required accuracy.

4.2. CrO_2

The results of our calculations for non-magnetic chromium dioxide are shown in figure 7 and in table 2. The first lower band, composed mainly of the oxygen 2s states and separated by a large gap from other bands, has been omitted. The oxygen 2p bands are thus the lowest ones shown. They are slightly mixed with the Cr 3d bands. Then, above a gap, we find the majority of the Cr 3d states. E_F lies in this region in a local minimum of the DOS. CrO_2 has a Stoner parameter of about 8, so the paramagnetic phase of CrO_2 is unstable. In order to estimate the equilibrium magnetic moment in the rigid-band approximation we have calculated the function $\overline{N(m)}$ (see figure 8). As in the case of NiMnSb, there is a step in the $\overline{N(m)}$ curve—here, at $2\mu_B$—due to the band gap between

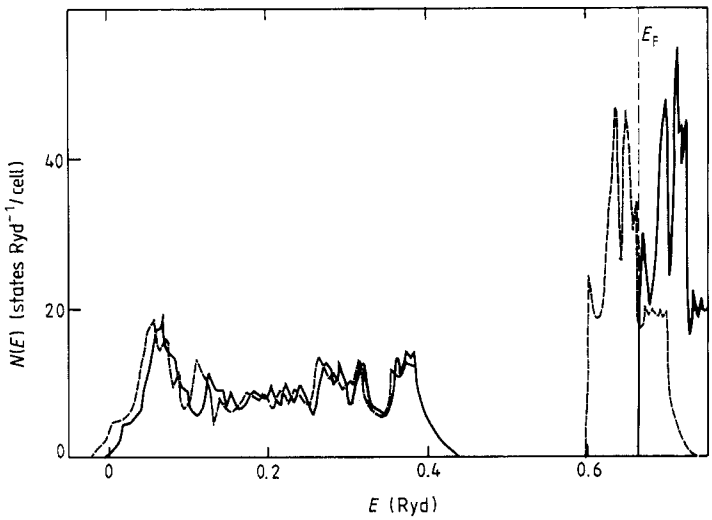

Figure 9. Density of states of ferromagnetic CrO_2. Broken traces show spin-down DOS.

the O 2p and Cr 3d bands. Only one stable phase was found. Spin-polarised calculations show (figure 9) that E_F is actually at the top of the gap, and not inside the gap, as ESFC predicts. However, the exact position of E_F depends on the exchange–correlation potential approximation.

5. Conclusions

NiMnSb and CrO_2 are examples of 'half-metallic' materials: they behave as 'metals' as regards the majority-spin bands and as 'semiconductors' as regards the minority-spin bands. This is correctly predicted by the extended Stoner factor calculations. Of particular interest is NiMnSb, where the conventional Stoner criterion fails completely ($I^*N(E_F) = 0$), but the ESFC give very reasonable results. The ESFC also predict a low-spin metastable state in NiMnSb with a magnetic moment of $m = 0.14\mu_B$. It is important to note that the position of the Fermi level in the gap is so sensitive to the exchange–correlation potential approximations that any conclusion about this position from the LDA calculations would be unreliable.

Acknowledgments

We acknowledge very helpful discussions with O K Andersen and O Gunnarsson. One of us (IIM) acknowledges the support of the Alexander-von-Humboldt Foundation.

References

Andersen O K 1975 *Phys. Rev.* B **12** 3060
Andersen O K, Madsen J, Poulsen U K, Jepsen O and Kollar J 1977 *Physica* B **86–88** 249
de Groot R A, Mueller F M, van Engen P G and Buschow K H J 1983 *Phys. Rev. Lett.* **50** 2024
—— 1984 *Appl. Phys.* **55** 2151

Gunnarsson O 1976 *J. Phys. F: Met. Phys.* **6** 587
Gunnarsson O and Lundqvist B I 1976 *Phys. Rev.* B **13** 4274
Janak J F, Moruzzi V L and Williams A R 1975 *Phys. Rev.* B **12** 1257
Kamper K P, Schmitt W, Guntherodt G, Gambino R J and Ruf R 1987 *Phys. Rev. Lett.* **59** 2788
Krasko G L 1987 *Phys. Rev.* B **36** 8565
Schwarz K 1986 *J. Phys. F: Met. Phys.* **16** L211
von Barth U and Hedin L 1972 *J. Phys. C: Solid State Phys.* **5** 1629
Vosko S H, Wilk L and Nussair M 1980 *Can. J. Phys.* **58** 1200
Watanabe K 1976 *Trans. Japan Inst. Met.* **17** 220